

## **Reassessment of antibody-based detection of the murine T cell GLP-1 receptor**

Chi Kin Wong<sup>1</sup>, Bernardo Yusta<sup>1</sup>, Jason CL Tong<sup>2</sup>, David J Hodson<sup>2</sup>, Daniel J Drucker<sup>1</sup>

### Affiliations

From the Lunenfeld-Tanenbaum Research Institute<sup>1</sup>, Mt. Sinai Hospital, Toronto ON Canada and the Oxford Centre for Diabetes, Endocrinology and Metabolism<sup>2</sup>, Oxford Centre for Diabetes, Endocrinology and Metabolism (OCDEM), NIHR Oxford Biomedical Research Centre, Churchill Hospital, Radcliffe Department of Medicine, University of Oxford, Oxford, UK.

### Correspondence and Lead Contact:

Daniel J Drucker  
LTRI, Sinai Health  
600 University Avenue Mailbox39  
Toronto Ontario M5G 1X5  
[drucker@lunenfeld.ca](mailto:drucker@lunenfeld.ca) V 416-361-2661

## Summary

Glucagon-like peptide 1 receptor (GLP-1R) agonists exert systemic anti-inflammatory effects, but the contribution of direct immune cell GLP-1R signalling remains uncertain. Although systemic T cell responses to GLP-1 have been reported, low receptor abundance and suboptimal antisera complicate efforts to determine the importance of GLP-1R signalling in T cells. Here, we evaluate 3 different antisera and show that a commonly used antibody AGR-021 lacks specificity for the GLP-1R in mice. Immunostaining with AGR-021 using tissues from two independent GLP-1R knockout mouse lines reveals persistent immunoreactive signals in GLP-1R-null pancreatic islets. Similarly, flow cytometry using AGR-021 reveals no reduction in AGR-021 immunoreactivity in GLP-1R-null splenic T cells. Moreover, Western blotting detects AGR-021- immunoreactive proteins from a GLP-1R-negative cell line and fails to detect immunoreactive GLP-1R of the correct size upon overexpression of the receptor. These findings challenge the validity of studies relying on this antibody to infer GLP-1R expression.

Key words: Reproducibility, antibodies, G protein-coupled receptors, inflammation, Glucagon-like peptide-1, T cells, immunohistochemistry, flow cytometry

## Introduction

There is tremendous interest in understanding how glucagon-like peptide 1 (GLP-1)-based medicines reduce inflammation<sup>1</sup>. Recent clinical trials show benefits for GLP-1 medicines in cardiovascular diseases<sup>2</sup> chronic kidney diseases<sup>3</sup>, metabolic dysfunction-associated steatohepatitis<sup>4</sup> and osteoarthritis<sup>5</sup>, disorders characterized by dysregulated immune responses. Emerging preclinical data suggest that GLP-1 medicines exert both local and systemic anti-inflammatory effects via direct actions on GLP-1R+ immune cells within the intestine and indirect actions via the central nervous system<sup>6,7</sup>. In the intestine, mouse intraepithelial lymphocytes (IELs) are one of the few T cell populations that robustly express GLP-1R and the activity of these cells is functionally suppressed by GLP-1R agonists in a receptor-dependent manner<sup>6,8</sup>. In contrast, primary immune organs such as the thymus and bone marrow, and secondary immune organs including the spleen and peripheral lymph nodes, express low levels of *Glp1r*<sup>6,8-10</sup>. Within these organs, *Glp1r* is likely expressed in selected immune cells, as inferred from studies using transgenic mice lacking *Glp1r* in Lck or Tie2-expressing lineages<sup>6,11</sup>.

A recent preclinical study explored the role of GLP-1R signalling in immune tolerance<sup>12</sup>. Mice lacking GLP-1R globally rejected BALB/c heart allografts more rapidly than wildtype controls. Similarly, daily injection of 2 µg exendin(9-39,) a GLP-1R antagonist, reduced tumor size in mice bearing MC38 syngeneic tumors, consistent with enhanced immune activation in the context of attenuated GLP-1R signalling. Conversely, treatment with exendin-4 (0.2 µg or 2 µg) twice daily for two weeks post-transplant delayed islet allograft rejection and modestly prolonged heart allograft survival<sup>12</sup>. These findings suggest that GLP-1R activation dampens T cell-mediated immune responses to promote tolerance, while its inhibition enhances immune activity. Although the specific immune cell types mediating these *in vivo* effects remain poorly defined, these results are consistent with prior findings demonstrating GLP-1R-dependent suppression of gut IEL activation<sup>6</sup>.

To identify the cell types responsible for these immunomodulatory effects of GLP-1R signalling, Ben Nasr and colleagues used a commercially available antibody (clone AGR-021, Alomone Labs), raised against the extracellular domain of rat GLP-1R, to detect immunoreactive GLP-1R expression in both mouse and human T cells. AGR-021 was used extensively to characterize GLP-1R<sup>+</sup> versus GLP-1R<sup>-</sup> T cells for downstream cellular and molecular analyses<sup>12</sup>. However, several issues and inconsistencies raise questions about the interpretation of data generated using the AGR-021 antibody.

First, levels of *Glp1r* mRNA transcripts are known to be very low in major immune organs including the spleen and thymus<sup>6,8-10</sup>, a finding that was confirmed using qPCR in the 2024 Cell Metabolism study<sup>12</sup>. The very low abundance of immune *Glp1r* expression contrasts with the widespread distribution of GLP-1R immunoreactivity reported across multiple splenic immune populations using the AGR-021 antibody<sup>12</sup>. Second, Western blot data using AGR-021 from experiments illustrated by the vendor (<https://www.alomone.com/p/anti-glucagon-like-peptide-1-receptor-extracellular/AGR-021?srsId=AfmBOorKxLkbvX5t3sB9-HFj5oL5vLXsvFiq-AGn7V9nVP54fxeRxBJa>), and

in the 2024 Cell Metabolism paper<sup>12</sup>, report a GLP-1R-immunoreactive band at 110 kDa but not at the expected molecular weight of the GLP-1R at ~55 kDa as previously detected in cells transfected with cDNAs encoding the GLP-1R<sup>13,14</sup>. Uncropped blot images produced using the AGR-021 antisera do not reveal a specific 55 kDa signal in either GLP-1R-overexpressing cell lines or in mouse T cells<sup>12</sup>. Third, in experiments assessing GLP-1R immunoreactivity in the mouse pancreas, AGR-021 yields diffuse, non-membrane-associated staining in regions that do not resemble islets, despite the known localization of the receptor in this organ. Collectively, these observations suggest that AGR-021 immunoreactivity may not faithfully report authentic GLP-1R expression. In the present study, we evaluated the sensitivity and specificity of AGR-021 using multiple complementary methods across two independent laboratories, and concluded that AGR-021 is neither sensitive nor specific for detecting mouse GLP-1R expression

## Results

### **AGR-021 immunoreactivity does not colocalize with fluorescent GLP-1R ligand signals in isolated mouse islets**

To assess the specificity of the GLP-1R antibody AGR-021, which has been used in multiple published studies to detect GLP-1R expression (Supplementary Table 1), we evaluated its performance using a range of complementary techniques across two laboratories. We first performed immunofluorescence staining on isolated pancreatic islets from whole body *Glp1r* knockout mice (*Glp1r*<sup>H-KO</sup>) generated via CRISPR-Cas9<sup>15</sup>. Pancreatic islets express high levels of GLP-1R, which can be reliably visualized using LUXendin645, a fluorescent exendin-9-39 peptide probe that binds GLP-1R with high specificity<sup>15</sup>. As expected, LUXendin645 produced membrane-associated fluorescence in wildtype islet cells (Figure 1A). We next tested the GLP-1R antibody ab218532, which showed strong colocalization with LUXendin645 in wildtype islets, yet no signal was detected in GLP-1R-null islets (Figures 1A and 1B). Therefore, we used ab218532 as a control in subsequent experiments. In contrast, AGR-021 produced sparse and inconsistent staining across islet cells with minimal overlap with LUXendin645 (Figure 1C). Critically, AGR-021 continued to generate diffuse cytoplasmic fluorescence signals in GLP-1R-null islets, whereas LUXendin645 did not label any cells in islets from *Glp1r*<sup>-/-</sup> mice (Figure 1D). Of note, insulin staining was much weaker in islets co-stained with AGR-021, suggesting some non-specific binding to, and competition for, insulin epitopes (Figure 1C and D).

### **AGR-021 immunoreactivity persists in tissues lacking GLP-1R**

We next assessed the AGR-021 antibody and ab218532 using immunohistochemistry on whole tissue sections from a second whole body GLP-1R knockout mouse line (*Glp1r*<sup>D-KO</sup>)<sup>16</sup>. In the wildtype pancreas, ab218532 produced robust staining restricted to islets, with no detectable signals in the exocrine pancreas (Figure 2A). This staining was markedly reduced in the GLP-1R-null pancreas, supporting the specificity of ab218532. In contrast, AGR-021 produced comparable staining patterns in both wildtype and GLP-1R-null pancreata, with signals present in both exocrine and endocrine compartments (Figure 2A). Within the islets, AGR-021 staining was primarily localized to the mantle

region that is typically enriched in non- $\beta$  cells in mice, further suggesting that its immunoreactivity may not reflect specific detection of GLP-1R.

We next tested antibody performance on tissue sections of Brunner's glands, which are known to express high levels of GLP-1R<sup>17</sup>. The ab218532 antibody predominantly stained secretory cells with a membrane-associated pattern consistent with GLP-1R localization (Figure 2B)<sup>18</sup>. Some non-specific staining was observed in mucus vacuoles of the gut epithelium in both wildtype and GLP-1R knockout mice. However, secretory cells in GLP-1R knockout mice lacked detectable ab218532 staining, supporting its specificity. In contrast, AGR-021 produced strong nuclear staining in both Brunner's glands and adjacent epithelium, with similar patterns in both control and GLP-1R-null tissues, indicating non-specific binding (Figure 2B).

We next tested these antibodies in mouse thymus sections, as recent studies with the AGR-021 antibody demonstrated numerous thymic cells with diffuse cytoplasmic GLP-1R-immunopositivity<sup>12</sup>. In wildtype thymus, ab218532 showed sparse staining in the medulla and none in the cortex (Figure 2C). Two morphologically distinct cell populations were labelled: one displaying the membrane-associated pattern and another with strong cytoplasmic signal. In GLP-1R-null thymus, membrane-associated staining was lost, while cytoplasmic staining persisted, suggesting the latter represents non-specific background (Figure 2C). In contrast, AGR-021 showed widespread staining across both cortex and medulla, with similar patterns observed in wildtype and GLP-1R-null tissues (Figure 2C). These findings indicate that AGR-021 lacks both sensitivity and specificity for detecting mouse GLP-1R by immunohistochemistry, whereas ab218532 demonstrates high sensitivity and moderate specificity across tissues.

### **Enrichment of AGR-021-immunoreactive splenic T cells**

The AGR-021 antibody has also been used in flow cytometry to identify GLP-1R<sup>+</sup> splenic T cells for functional and transcriptomics analyses<sup>12,19</sup>. To assess whether AGR-021 is sufficiently sensitive to enrich for GLP-1R<sup>+</sup> cells and specific enough to exclude GLP-1R<sup>-</sup> cells, we performed flow cytometry on live splenic T cells from wildtype and GLP-1R-null mice. AGR-021 labelled a small subset of both CD4<sup>+</sup> and CD8<sup>+</sup> splenic T cells relative to fluorescence-minus-one controls (Figures 3A and 3B). Importantly, the frequencies of AGR-021<sup>+</sup> T cells were identical between wildtype and GLP-1R-null spleens.

Given the very low level of *Glp1r* expression in spleen<sup>7,8,11,12</sup> we next tested whether AGR-021 could detect GLP-1R<sup>+</sup> T cells in gut intraepithelial lymphocytes (IELs), a cell type known to robustly express *Glp1r*<sup>6,8</sup>. Similar to findings obtained with splenic tissue, AGR-021 bound comparable fractions of CD8<sup>+</sup> IELs in wildtype and GLP-1R-null mice (Figure 3C). We also tested ab218532, but it produced no flow cytometry signals on splenocytes (Supplementary Figure 2). Another monoclonal antibody frequently used to detect GLP-1R expression, 7F38<sup>20</sup>, labelled a small population of splenic T cells and IELs, but the frequency of 7F38<sup>+</sup> T cells was also indistinguishable between wildtype and GLP-1R-null mice (Figures 3D and 3E).

To determine whether AGR-021<sup>+</sup> cells express *Glp1r*, we magnetically enriched CD90<sup>+</sup> splenic T cells and performed fluorescence-activated cell sorting (FACS) to isolate AGR-021<sup>+</sup> and AGR-021<sup>-</sup> CD4<sup>+</sup> and CD8<sup>+</sup> populations. CD90<sup>+</sup> splenic T cells expressed higher levels of *Glp1r* than bulk splenocytes by qPCR (Figure 3F). All sorted T cell populations expressed high levels of *Cd3g*, although AGR-021<sup>+</sup> T cells exhibited lower levels of *Cd3g* than AGR-021<sup>-</sup> counterparts (Figure 3G). Notably, AGR-021<sup>+</sup> CD4<sup>+</sup> T cells expressed *Glp1r*, whereas AGR-021<sup>+</sup> CD8<sup>+</sup> T cells did not (Figure 3F). Together, these results suggest that AGR-021 lacks the specificity for reliable detection of GLP-1R in mouse T cells by flow cytometry.

### **AGR-021 fails to detect mouse GLP-1R at the expected molecular weight**

Previous studies using AGR-021 reported detection of an immunoreactive GLP-1R protein in extracts from murine CD4 and CD8 cells, as well as islets with a molecular weight of 110 kDa<sup>12</sup>. To assess whether AGR-021 can detect the authentic mouse GLP-1R by Western blotting, we probed lysates from cells overexpressing mouse GLP-1R with AGR-021 (Figure 4A) and ab218532 (Figure 4B) as previously described<sup>14</sup>. AGR-021 produced multiple (at least 6) bands in both control lysates as well as those prepared from cells with enhanced GLP-1R expression (Figure 4A). While a 110 kDa band was visible as previously reported<sup>12</sup>, no signal was observed at 55 kDa, which is the expected molecular weight of mouse GLP-1R<sup>14</sup>. In contrast, ab218532 produced a strong 55 kDa band in GLP-1R-overexpressing cells, but no such band in control lysates (Figure 4B). GAPDH levels were comparable across the transfected cell lysates (Figure 4C). Taken together, these findings indicate that AGR-021 lacks both sensitivity and specificity for detecting mouse GLP-1R by Western blotting.

### **Discussion**

There is strong interest in developing and validating GLP-1R-specific antibodies for mouse and human applications, driven by the expanding field of GLP-1 physiology and pharmacology. However, detecting native G protein-coupled receptors (GPCRs) using antibodies remains challenging due to their typically low and variable cell surface expression<sup>21,22</sup>. Notably, insufficient antibody specificity is a common problem in biomedical research, with more than 50% of 614 commercial antibodies failing one or more tests of antibody validation<sup>23</sup>. Many commercially available GPCR-targeting antibodies lack sufficient sensitivity and specificity<sup>14,24</sup>, and several GLP-1R antibodies have been invalidated using tissues from GLP-1R knockout mice<sup>14,25</sup>. The widespread use of GLP-1R antibodies that lack specificity raises significant concerns about the reproducibility and reliability of data inferring localization of the GLP-1R, a drug target of expanding importance<sup>10,26</sup>.

Here, we found that the AGR-021 antibody is neither specific nor sensitive for detecting mouse GLP-1R, based on experiments independently conducted in two laboratories, using two different lines of GLP-1R knockout mice as controls for antibody specificity. Across a range of commonly used techniques such as immunofluorescence, immunohistochemistry, flow cytometry, and Western blotting, AGR-021 performed poorly relative to ab218532, which we validated for all applications except flow cytometry. AGR-021 lacks specificity, as it produces signals even in GLP-1R-null

tissues and cell lines that do not express the GLP-1R. It also lacks sensitivity, failing to produce membrane-associated staining in pancreatic  $\beta$  cells and failing to detect a 55 kDa band in Western blotting, even in extracts from transfected cells with high levels of GLP-1R expression.

Our findings further underscore that the performance of GLP-1R antibodies is highly assay- and tissue-dependent. For example, ab218532 is suitable for immunohistochemistry, immunofluorescence, and Western blotting, but is ineffective in flow cytometry. 7F38 was also validated for immunohistochemistry. This limitation is compounded by its lack of direct fluorophore conjugation, which prevents straightforward use in flow-based applications. Moreover, the very low endogenous levels of *Glp1r* in spleen and thymus challenges the limits of detection in flow cytometry. Although most ab218532 signals were absent in the Brunner's glands and thymus of GLP-1R-null mice in immunohistochemistry experiments, this antibody exhibited some background staining in these tissues. These observations highlight the need for rigorous, context-specific antibody validation and caution when interpreting unvalidated or marginal findings.

Given the lack of specificity of AGR-021, it remains unclear whether peripheral conventional T cells express GLP-1R at functionally meaningful levels. We observed higher *Glp1r* transcript levels in CD90<sup>+</sup> splenocytes than in CD90<sup>-</sup> cells, suggesting that T cells may contribute a greater share of splenic *Glp1r* expression. In addition, AGR-021<sup>+</sup> CD4<sup>+</sup> T cells showed enrichment of *Glp1r* transcripts, whereas AGR-021<sup>+</sup> CD8<sup>+</sup> T cells did not. It is possible that AGR-021 binds an unrelated antigen expressed by a subset of T cells that coincidentally also express *Glp1r*, rather than specifically recognizing GLP-1R. We interpret this enrichment as coincidental for several reasons: 1) AGR-021 fails specificity and sensitivity tests across immunohistochemistry, immunofluorescence, and Western blotting; 2) it produces flow cytometry signals in GLP-1R-null splenic T cells and IELs; and 3) AGR-021<sup>-</sup> CD4<sup>+</sup> and AGR-021<sup>-</sup> CD8<sup>+</sup> T cells still express detectable *Glp1r* transcripts. These findings suggest that a subset of CD4<sup>+</sup> T cells may genuinely express *Glp1r*, independent of AGR-021 staining. Notably, CD4<sup>+</sup> splenic T cells expressing high levels of *Glp1r* transcripts may include regulatory T cells (Tregs), one of the few splenic immune populations known to express full-length *Glp1r* mRNA<sup>9</sup> and a plausible target through which GLP-1R signalling could modulate immune tolerance.

The field of GLP-1 therapeutics is well established in the context of T2D and obesity<sup>27</sup>, yet has expanded rapidly with recent success in trials of metabolic liver disease, osteoarthritis, chronic kidney disease, and atherosclerotic cardiovascular disease, disorders collectively characterized by dysregulated inflammation<sup>1</sup>. Moreover, ongoing clinical trials are assessing the therapeutic potential of GLP-1 medicines in people with type 1 diabetes (NCT069148950), psoriatic arthritis (NCT06864026), Crohn's disease (NCT06937099) and Alzheimer's disease<sup>28</sup>, conditions similarly characterized by substantial alterations in immune function. Hence, assessment of how GLP-1 medicines directly modify GLP-1R signalling in immune cells has important translational implications for understanding the safety and anti-inflammatory actions of GLP-1

medicines across a range of human diseases. Although several recent papers describe exciting actions for GLP-1 medicines in the modulation of experimental T cell function, the utility of the data generated using the AGR-021 antibody for isolation and identification of the putative GLP-1R+ T cells in these papers <sup>12,19</sup> is challenged by the major limitations of this reagent identified herein. Taken together, the data presented here reinforces the ongoing importance of vigilance and reagent validation for ensuring accuracy and reproducibility in studies assessing GPCR expression and functional activity <sup>26</sup>.

## Acknowledgments

D.J.D. is supported, in part, by a Banting and Best Diabetes Centre–Novo Nordisk Chair in Incretin Biology, a Sinai Health–Novo Nordisk Foundation Fund in Regulatory Peptides, CIHR grants 154321 and 19204 and Diabetes Canada-Canadian Cancer Society grant (OG-3- 24-5819-DD). D.J.H. was supported by MRC (MR/S025618/1), Diabetes UK (22/0006389) and UKRI ERC Frontier Research Guarantee (EP/X026833/1) Grants. This work was supported on behalf of the “Steve Morgan Foundation Type 1 Diabetes Grand Challenge” by Diabetes UK and SMF (grant number 23/0006627).

## Conflicts of Interest

DJD has received consulting fees from Alnylam, Amgen, AstraZeneca Inc., Crinetics, Insulet, Kallyope, Metsara, and Pfizer Inc. and speaking fees from Novo Nordisk Inc. Mount Sinai Hospital, has received investigator-initiated grant support from Amgen, Eli Lilly Inc., Novo Nordisk, Pfizer and Zealand Pharmaceuticals Inc. to support preclinical studies in the Drucker laboratory. D.J.H. has filed a patent on GLP1R and GIPR chemical probes. D.J.H. receives licensing revenue from Celtarys Research for provision of GLP1R/GIPR chemical probes. D.J.H. has filed patents related to type 2 diabetes therapy and GLP1R agonism.



## Methods

### Animals

All animal procedures were approved by the Animal Care and Use Subcommittee at the Toronto Centre for Phenogenomics at Mount Sinai Hospital (Toronto, Canada), and by the Animal Welfare and Ethical Review Body (AWERB) at the University of Oxford. Mice were housed in groups of up to five per cage in holding rooms with lights on between 7 am to 7 pm, with ad libitum access to water and standard chow. *Glp1r<sup>H-KO</sup>* mice were generated using a CRISPR-Cas9 approach<sup>15</sup>, and *Glp1r<sup>D-KO</sup>* mice were produced by traditional homologous recombination<sup>16</sup>.

### LUXendin-Based GLP-1R Labelling and Immunofluorescence Staining of Mouse Islets

Size-matched islets were incubated with LUXendin645 (500 nM) for 1 hour at 37 °C in 5% CO<sub>2</sub> as previously described<sup>15</sup>. Following labelling, islets were fixed in 10% formalin at room temperature for 15 minutes. Fixed islets were then incubated at 4°C overnight with primary antibodies diluted in blocking buffer (2% BSA, 0.2% Triton X-100 in PBS), followed by incubation with secondary antibodies in the same buffer. Nuclei were stained with 1 µg/mL Hoechst 33342 (Thermo Fisher Scientific, cat no. H3570) for 15 minutes before mounting with ProLong Glass Antifade Mountant (Thermo Fisher Scientific, cat no. P36982). The primary antibodies used included: 1:5 guinea pig anti-insulin (Dako, cat no. A056401-2-2; RRID: AB\_2617169), 1:2000 mouse anti-glucagon (Sigma-Aldrich, cat no. G2654; RRID:AB\_259852), 1:1000 rabbit anti-GLP-1R (Abcam, cat no. ab218532, RRID: AB\_2864762) and 1:200 rabbit anti-GLP-1R (Alomone, cat no. AGR-021, RRID:AB\_10917158). Secondary antibodies included: 1:1000 donkey anti-rabbit Alexa Fluor 488 (Thermo Fisher Scientific, cat no. A-21206, RRID: AB\_2535792), 1:1000 goat anti-guinea pig Alexa Fluor 568 (Thermo Fisher Scientific, cat no. A-11075, RRID: AB\_2534119) and 1:1000 goat anti-mouse Alexa Fluor 647 (Abcam, cat no. ab150119, RRID: AB\_2811129). Imaging was performed using an Olympus FV4000 confocal microscope equipped with highly-sensitive SiVIR spectral detectors and 40x, 0.95 NA and 60x, 1.42 NA UPLSAPO oil immersion objectives. Identical microscope settings (laser power, detector %) were used for all samples, with brightness and contrast adjustments applied equally for presentation purposes.

### Immunohistochemistry

Pancreas, Brunner's gland, and thymus tissues were fixed in 10% formalin at room temperature for 24 hours, followed by serial dehydration in ethanol and xylene. Dehydrated tissues were embedded in paraffin and sectioned at a thickness of 4 µm. Sections were rehydrated with xylene, ethanol, and water, then subjected to antigen retrieval in TE pH 9.0 at 95°C for 40 minutes in a decloaking chamber (Biocare Medical). After cooling, sections were then blocked with blocking buffer (10% goat serum and 0.1% Triton X-100 in TBST) at room temperature for 30 minutes. Primary antibodies were applied overnight at 4°C. Slides were then washed three times 5 minutes each in TBST, followed by incubation with horseradish peroxidase (HRP)-based SignalStain Boost IHC Detection Reagent (Cell Signalling Technology, 8114S) at room temperature for 1 hour. Primary antibodies used were rabbit anti-GLP1R ab218532 at 1/500 (Abcam) and rabbit anti-GLP1R AGR-021 at 1/200 (Alomone Labs).

After a further three washes in TBST, chromogenic signal development was performed using the Impact DAB substrate kit (Vector Laboratories) for 2 minutes. Slides were counterstained with haematoxylin QS diluted 1:10 in water for 30 seconds (Vector Laboratories), mounted with Prolong Gold Antifade Mountant (Thermon), and scanned at 20x magnification using a Zeiss Axio scan 7 slide scanner (Zeiss).

### **Magnetic Cell Sorting of CD90<sup>+</sup> Splenic T cells**

Splenocytes were isolated by gently mashing spleens through a 70- $\mu$ m cell strainer with a syringe plunger into RPMI 1640 medium (Wisent) supplemented with 10% fetal bovine serum (FBS; Wisent) and penicillin/streptomycin (Thermon). Cells were washed once with RPMI, then incubated on ice with mouse FcR blocking reagent (Miltenyi) for 10 minutes. Magnetic separation was performed using anti-CD90.2 microbeads (Miltenyi) and LS columns (Miltenyi) according to the manufacturer's protocol. The enriched CD90<sup>+</sup> splenic T cells were subsequently used for flow cytometry or FACS experiments.

### **Isolation of Intraepithelial Lymphocytes (IELs)**

IELs were isolated from the small intestine as previously described<sup>6</sup>. Small intestines were cut into 1-cm pieces, washed with HBSS without calcium/magnesium, and incubated in RPMI 1640 supplemented with 10% FBS (Wisent) and penicillin/streptomycin, 10 mM HEPES (Thermo), and 1 mM DTT (Bioshop) at 37°C for 40 minutes. Tissues were then centrifuged at 500 g for 5 minutes and resuspended in 10 mL of the same supplemented RPMI without DTT. The samples vortexed vigorously for 3 minutes, and the supernatant was collected by passing through a 100- $\mu$ m cell strainer. The tissues remaining on the strainer were further vortexed in 10 mL medium and filtered again through the 100- $\mu$ m cell strainer. The combined supernatant was top up to 40 mL with medium and centrifuged at 500 g for 5 minutes. The cell pellet was resuspended in 8 mL of 36% Percoll (GE Healthcare) and carefully layered over 67% Percoll (GE Healthcare). The gradient was centrifuged at 700 g for 20 minutes without acceleration or brake. Cells at the interface were collected, washed once with FACS buffer (25 mM HEPES, 2 mM EDTA, 1% FBS in PBS), and resuspended in FACS buffer. Percoll-purified IELs were sorted on a MA800 cell sorter (Sony) equipped with a 100- $\mu$ m nozzle, using forward and side scattering profiles and DAPI (Thermo) to gate live lymphocytes. The sorted IEL population was consistently >90% viable and >90% CD3<sup>+</sup> and was used for subsequent flow cytometry experiments.

### **Flow Cytometry and Fluorescence-Activated Cell Sorting (FACS)**

Splenic T cells or IELs were adjusted to  $1 \times 10^6$  cells/100  $\mu$ L and blocked with anti-CD16/CD32 antibody (Biolegend) on ice for 10 minutes. Cells were then incubated with on ice for 30 minutes with 3  $\mu$ g of one of the following antibodies diluted in FACS buffer: rabbit anti-GLP1R AGR-021 (Alomone Labs), mouse anti-GLP1R 7F38 (Novo Nordisk), or rabbit anti-GLP1R ab218532 (Abcam). After washing with FACS buffer, cells were incubated on ice for 30 minutes with Alexa Fluor 488-conjugated anti-rabbit IgG or anti-mouse IgG secondary antibodies (Thermo), along with PE-conjugated anti-CD4 (Biolegend) and APC-conjugated anti-CD8a antibodies (Biolegend). Following a final wash, cells were stained with DAPI and analyzed on a Gallios cytometer (Beckman Coulter). Data analysis was performed using Kaluza Analysis 2.1 software (Beckman

Coulter). For FACS sorting, AGR-021-stained splenic T cells were sorted on a Sony MA900 cell sorter into AGR-021<sup>+</sup> and AGR-021<sup>-</sup> CD4<sup>+</sup> and CD8<sup>+</sup> T cell populations.

### **Western Blotting**

BHK cells transfected with a pcDNA3.1 construct containing full-length mouse *Glp1r* cDNA were previously described<sup>14</sup>. Cells were lysed in Laemmli buffer and incubated at 37°C for 1 hour. Lysates containing 30 µg of total protein were resolved on 4-10% SDS-PAGE gels (Biorad) at 100 V. Proteins were transferred onto PVDF membranes at a constant current of 350 mA and 4°C for 90 minutes. Membranes were blocked with 5% BSA in TBST, followed by overnight incubation at 4°C with primary antibodies diluted in blocking buffer. Primary antibodies included rabbit anti-GLP1R ab218532 at 1/1000 (Abcam), rabbit anti-GLP1R AGR-021 at 1/1000 (Alomone Labs), and rabbit anti-GAPDH at 1/2000 (CST). Blots were washed three times with TBST and incubated with HRP-conjugated anti-rabbit IgG secondary antibody (CST) at room temperature for 1 hour. After three additional washes, membranes were incubated with SuperSignal West Pico PLUS chemiluminescent substrate (Thermo) for 5 minutes and imaged using a ChemiDoc imaging system (Biorad) with exposure time up to 2 minutes.

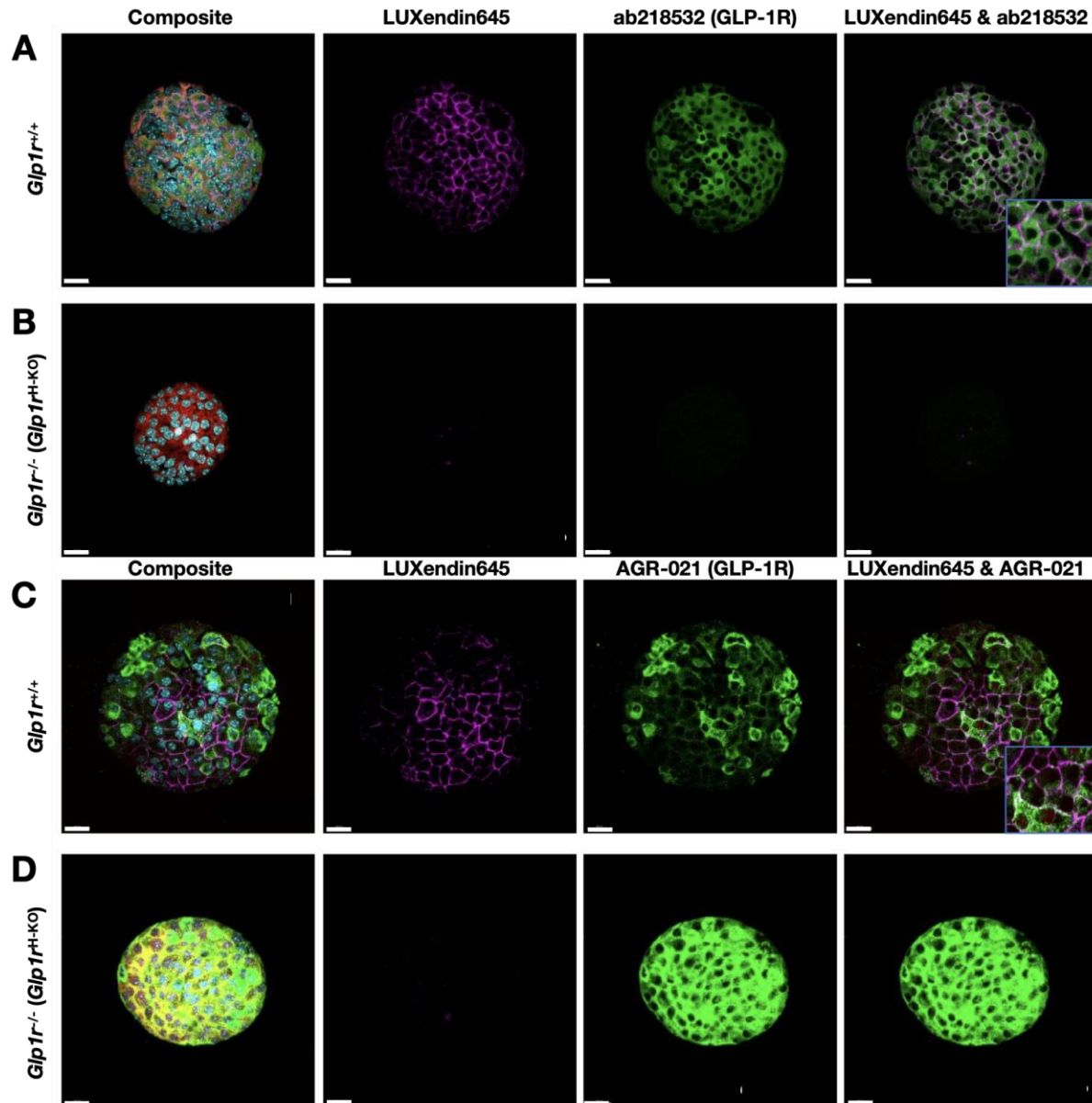


**Figure 1. Fluorescence-based detection of GLP-1R in isolated mouse islets using LUXendin-4, AGR-021, and ab218532.**

(A and B) Isolated islets from (A) *Glp1r*<sup>+/+</sup> and (B) *Glp1r*<sup>-/-</sup> (*Glp1r*<sup>H-KO</sup>) mice showing GLP-1R labelling with ab218532 and LUXendin645. Scale bar = 20  $\mu$ m. n = 3.

(C and D) Isolated islets from (C) *Glp1r*<sup>+/+</sup> and (D) *Glp1r*<sup>-/-</sup> mice showing GLP-1R labelling with AGR-021 and LUXendin645. Scale bar = 20  $\mu$ m. n = 3.

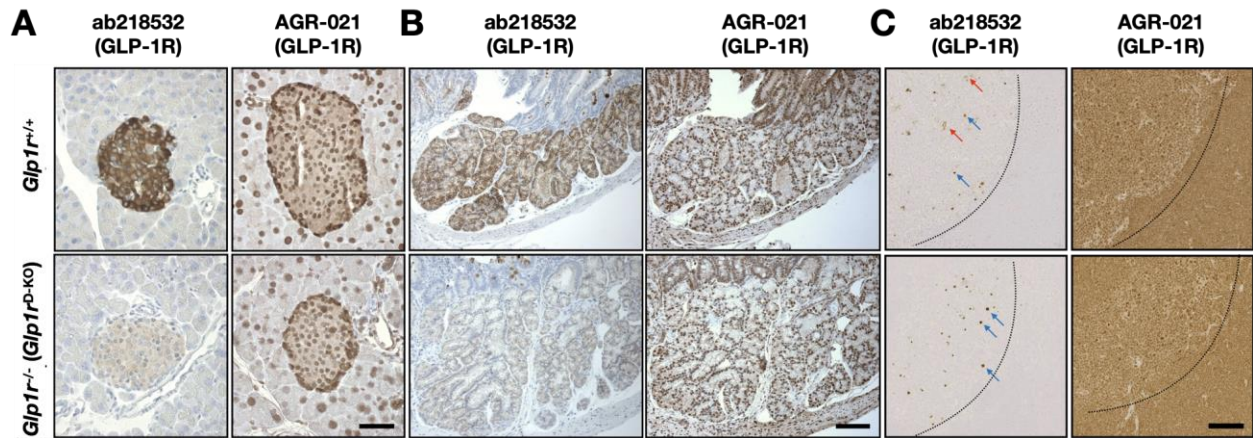


**Figure 2. Immunohistochemical detection of GLP-1R using AGR-021 and ab218532 in mouse pancreas, Brunner's glands, and thymus.**

(A, B and C) Immunohistochemistry staining of ab218532 or AGR-021 in the (A) mouse pancreas, (B) Brunner's gland, and (C) thymus, counterstained with haematoxylin. Scale bar = 50  $\mu$ m for Figure 2A, 100  $\mu$ m for Figures 2B and 2C. n = 4 from two independent experiments.

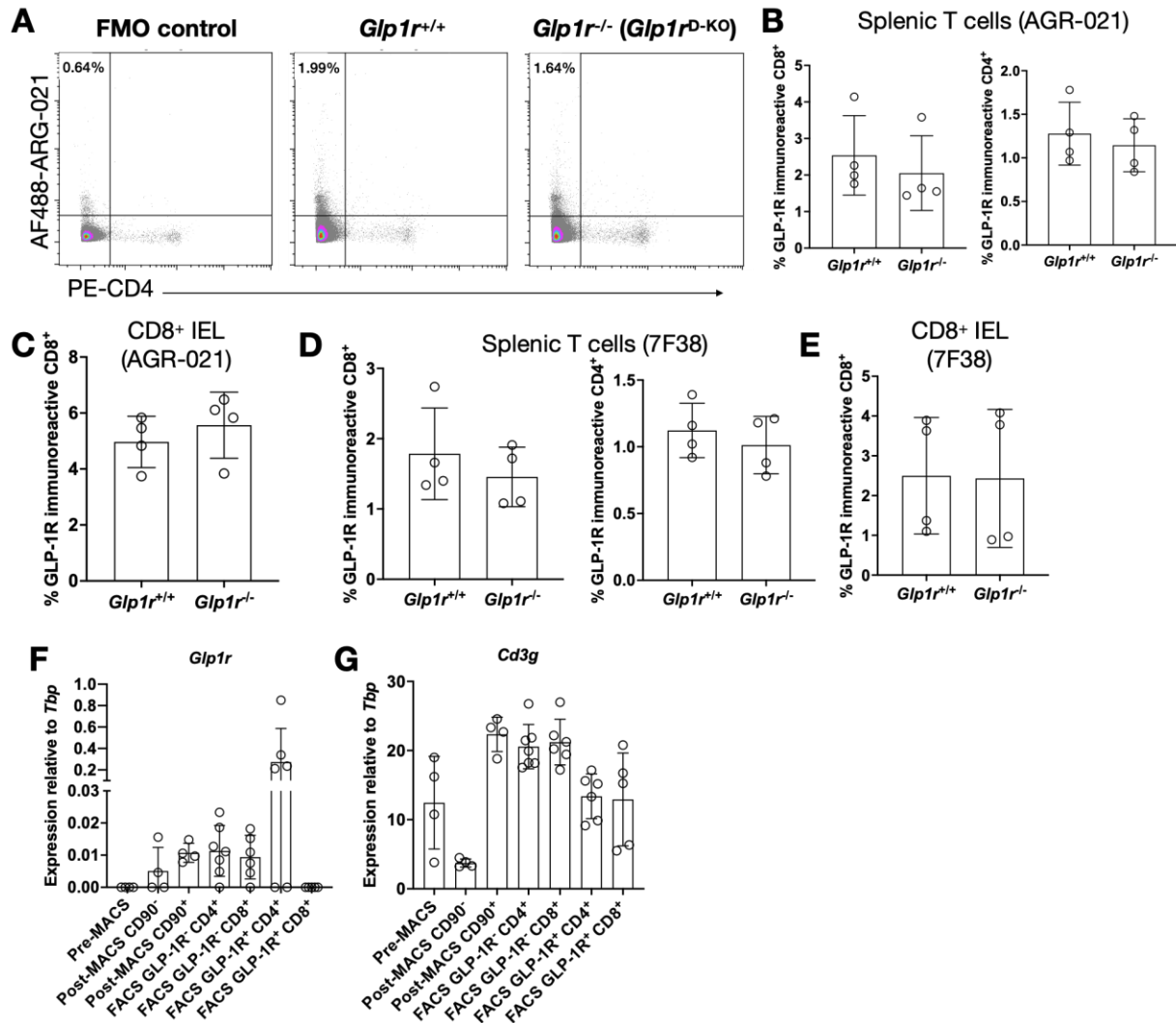


**Figure 3. Flow cytometry-based detection of AGR-021-labelled splenic T cells and IELs.**

(A) Representative density plots of CD8<sup>+</sup> splenic T cells stained with AGR-021 and CD4. AGR-021<sup>+</sup> CD4<sup>-</sup> populations (the gate with numeric percentages shown) were quantified as shown in Figure 3B. Data are gated on DAPI<sup>-</sup> CD8<sup>+</sup> populations.

(B) Bar plots showing the frequencies of AGR-021<sup>+</sup> CD8<sup>+</sup> CD4<sup>-</sup> (left panel) and AGR-021<sup>+</sup> CD8<sup>-</sup> CD4<sup>+</sup> (right panel) splenic T cells. n = 4. Data are pooled from two independent experiments.

(C) Bar plots showing the frequencies of AGR-021<sup>+</sup> CD8<sup>+</sup> CD4<sup>-</sup> IELs. n = 4. Data are pooled from two independent experiments.

(D) Bar plots showing the frequencies of 7F38<sup>+</sup> CD8<sup>+</sup> CD4<sup>-</sup> (left panel) and 7F38<sup>+</sup> CD8<sup>-</sup> CD4<sup>+</sup> (right panel) splenic T cells. n = 4. Data are pooled from two independent experiments.

(E) Bar plots showing the frequencies of 7F38<sup>+</sup> CD8<sup>+</sup> CD4<sup>-</sup> IELs. n = 4. Data are pooled from two independent experiments.

(F and G) qPCR analysis of (F) *Glp1r* and (G) *Cd3g* expression in pre-MACS (bulk splenocytes), MACS-purified CD90<sup>+</sup> and CD90<sup>-</sup> cells, and FACS-purified AGR-021<sup>-</sup> or AGR-021<sup>+</sup> CD4<sup>+</sup> and CD8<sup>+</sup> T cells. n = 4 - 6. Data are pooled from three independent experiments.

FMO = fluorescence-minus-one; MACS = magnetic-activated cell sorting; FACS = fluorescence-activated cell sorting

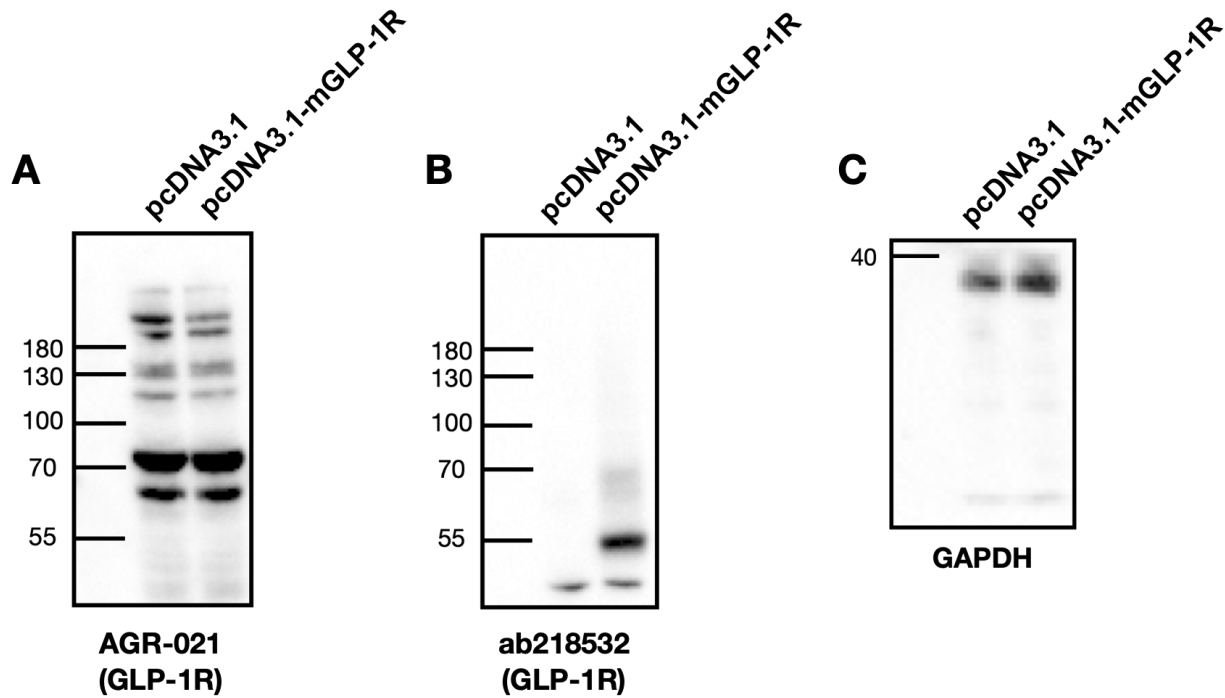
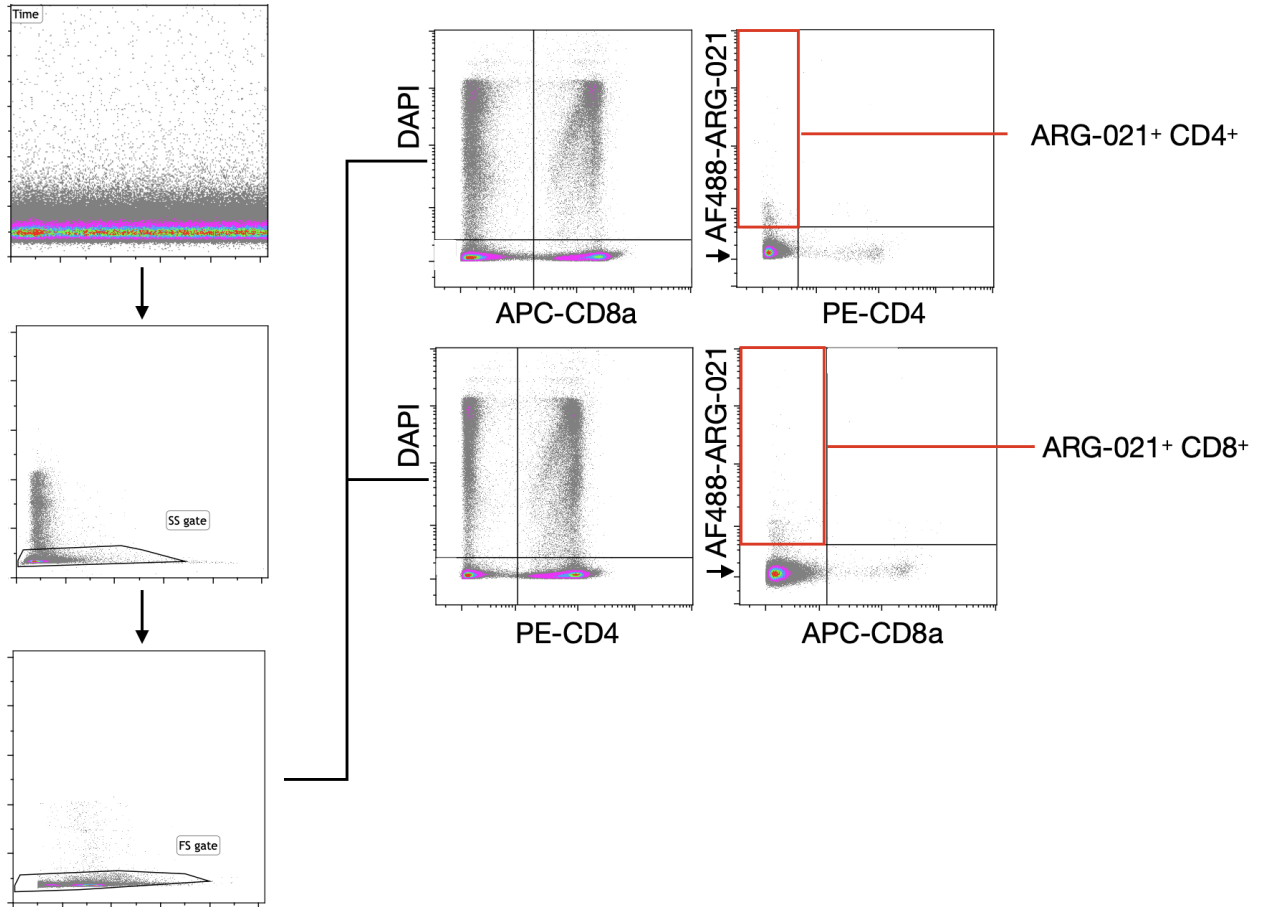
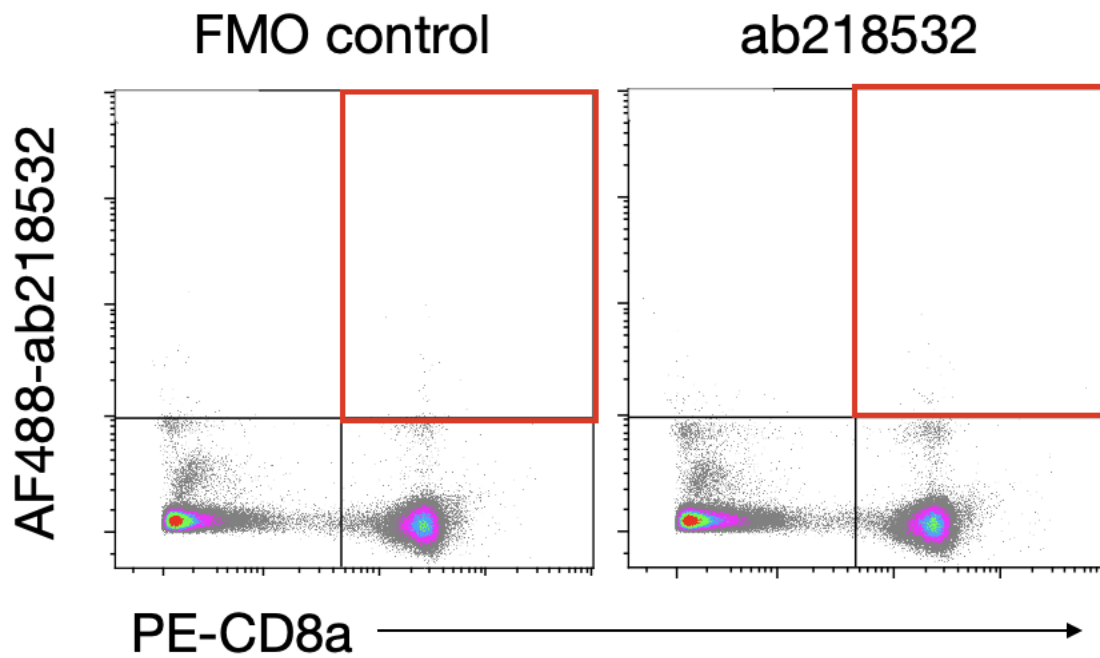


**Figure 4. Western blot detection of overexpressed mouse GLP-1R using AGR-021 and ab218532 antibodies.**

(A, B, and C) Lysates of cells transfected with either empty vector (pcDNA3.1) or pcDNA3.1 containing full-length mouse *Glp1r* cDNA were probed with (A) AGR-021, (B) ab218532, or (C) anti-GAPDH as a loading control. The experiment was independently repeated twice.



Supplementary Figure 1. Gating strategies for ARG-021<sup>+</sup> splenic T cells.



**Supplemental Figure 2. Flow cytometry analysis of splenic T cells labelled with ab218532.**

Red boxes indicate the ab218532<sup>+</sup> CD8<sup>+</sup> populations, which were not detectable.

1. Drucker, D.J. (2024). The benefits of GLP-1 drugs beyond obesity. *Science* 385, 258-260. 10.1126/science.adn4128.
2. Lincoff, A.M., Brown-Frandsen, K., Colhoun, H.M., Deanfield, J., Emerson, S.S., Esbjerg, S., Hardt-Lindberg, S., Hovingh, G.K., Kahn, S.E., Kushner, R.F., et al. (2023). Semaglutide and Cardiovascular Outcomes in Obesity without Diabetes. *The New England journal of medicine* 389, 2221-2232. 10.1056/NEJMoa2307563.
3. Perkovic, V., Tuttle, K.R., Rossing, P., Mahaffey, K.W., Mann, J.F.E., Bakris, G., Baeres, F.M.M., Idorn, T., Bosch-Traberg, H., Lausvig, N.L., et al. (2024). Effects of Semaglutide on Chronic Kidney Disease in Patients with Type 2 Diabetes. *The New England journal of medicine* 391, 109-121. 10.1056/NEJMoa2403347.
4. Sanyal, A.J., Newsome, P.N., Kliers, I., Ostergaard, L.H., Long, M.T., Kjaer, M.S., Cali, A.M.G., Bugianesi, E., Rinella, M.E., Roden, M., et al. (2025). Phase 3 Trial of Semaglutide in Metabolic Dysfunction-Associated Steatohepatitis. *The New England journal of medicine*. 10.1056/NEJMoa2413258.
5. Bliddal, H., Bays, H., Czernichow, S., Udden Hemmingsson, J., Hjelmessaeth, J., Hoffmann Morville, T., Koroleva, A., Skov Neergaard, J., Velez Sanchez, P., Wharton, S., et al. (2024). Once-Weekly Semaglutide in Persons with Obesity and Knee Osteoarthritis. *The New England journal of medicine* 391, 1573-1583. 10.1056/NEJMoa2403664.
6. Wong, C.K., Yusta, B., Koehler, J.A., Baggio, L.L., McLean, B.A., Matthews, D., Seeley, R.J., and Drucker, D.J. (2022). Divergent roles for the gut intraepithelial lymphocyte GLP-1R in control of metabolism, microbiota, and T cell-induced inflammation. *Cell metabolism* 34, 1514-1531 e1517. 10.1016/j.cmet.2022.08.003.
7. Wong, C.K., McLean, B.A., Baggio, L.L., Koehler, J.A., Hammoud, R., Rittig, N., Yabut, J.M., Seeley, R.J., Brown, T.J., and Drucker, D.J. (2024). Central glucagon-like peptide 1 receptor activation inhibits Toll-like receptor agonist-induced inflammation. *Cell metabolism* 36, 130-143 e135. 10.1016/j.cmet.2023.11.009.
8. Yusta, B., Baggio, L.L., Koehler, J., Holland, D., Cao, X., Pinnell, L.J., Johnson-Henry, K.C., Yeung, W., Surette, M.G., Bang, K.A., et al. (2015). GLP-1 receptor (GLP-1R) agonists modulate enteric immune responses through the intestinal intraepithelial lymphocyte (IEL) GLP-1R. *Diabetes* 64, 2537-2549. 10.2337/db14-1577.
9. Hadjiyanni, I., Siminovitch, K.A., Danska, J.S., and Drucker, D.J. (2010). Glucagon-like peptide-1 receptor signalling selectively regulates murine lymphocyte proliferation and maintenance of peripheral regulatory T cells. *Diabetologia* 53, 730-740.
10. McLean, B.A., Wong, C.K., Campbell, J.E., Hodson, D.J., Trapp, S., and Drucker, D.J. (2021). Revisiting the Complexity of GLP-1 Action from Sites of Synthesis to Receptor Activation. *Endocrine reviews* 42, 101-132. 10.1210/edrev/bnaa032.
11. McLean, B.A., Wong, C.K., Kaur, K.D., Seeley, R.J., and Drucker, D.J. (2021). Differential importance of endothelial and hematopoietic cell GLP-1Rs for cardiometabolic versus hepatic actions of semaglutide. *JCI insight* 6. 10.1172/jci.insight.153732.
12. Ben Nasr, M., Usuelli, V., Dellepiane, S., Seelam, A.J., Fiorentino, T.V., D'Addio, F., Fiorina, E., Xu, C., Xie, Y., Balasubramanian, H.B., et al. (2024). Glucagon-like peptide

- 1 receptor is a T cell-negative costimulatory molecule. *Cell metabolism* 36, 1302-1319 e1312. 10.1016/j.cmet.2024.05.001.
13. Baggio, L.L., Yusta, B., Mulvihill, E.E., Cao, X., Streutker, C.J., Butany, J., Cappola, T.P., Margulies, K.B., and Drucker, D.J. (2018). GLP-1 Receptor Expression Within the Human Heart. *Endocrinology* 159, 1570-1584. 10.1210/en.2018-00004.
  14. Panjwani, N., Mulvihill, E.E., Longuet, C., Yusta, B., Campbell, J.E., Brown, T.J., Streutker, C., Holland, D., Cao, X., Baggio, L.L., and Drucker, D.J. (2013). GLP-1 Receptor Activation Indirectly Reduces Hepatic Lipid Accumulation But Does Not Attenuate Development of Atherosclerosis in Diabetic Male ApoE<sup>-/-</sup> Mice. *Endocrinology* 154, 127-139. 10.1210/en.2012-1937.
  15. Ast, J., Arvaniti, A., Fine, N.H.F., Nasteska, D., Ashford, F.B., Stamataki, Z., Koszegi, Z., Bacon, A., Jones, B.J., Lucey, M.A., et al. (2020). Super-resolution microscopy compatible fluorescent probes reveal endogenous glucagon-like peptide-1 receptor distribution and dynamics. *Nature communications* 11, 467. 10.1038/s41467-020-14309-w.
  16. Scrocchi, L.A., Brown, T.J., McClusky, N., Brubaker, P.L., Auerbach, A.B., Joyner, A.L., and Drucker, D.J. (1996). Glucose intolerance but normal satiety in mice with a null mutation in the glucagon-like peptide 1 receptor gene. *Nature medicine* 2, 1254-1258. 10.1038/nm1196-1254.
  17. Bang-Berthelsen, C.H., Holm, T.L., Pyke, C., Simonsen, L., Sokilde, R., Pociot, F., Heller, R.S., Folkersen, L., Kvist, P.H., Jackerott, M., et al. (2016). GLP-1 Induces Barrier Protective Expression in Brunner's Glands and Regulates Colonic Inflammation. *Inflamm Bowel Dis* 22, 2078-2097. 10.1097/MIB.0000000000000847.
  18. Pyke, C., Heller, R.S., Kirk, R.K., Orskov, C., Reedtz-Runge, S., Kaastrup, P., Hvelplund, A., Bardram, L., Calatayud, D., and Knudsen, L.B. (2014). GLP-1 receptor localization in monkey and human tissue; Novel distribution revealed with extensively validated monoclonal antibody. *Endocrinology* 155, 1280-1290. 10.1210/en.2013-1934.
  19. Wu, J., Qian, P., Han, Y., Xu, C., Xia, M., Zhan, P., Wei, J., and Dong, J. (2025). GLP1 alleviates oleic acid-propelled lipocalin-2 generation by tumor-infiltrating CD8(+) T cells to reduce polymorphonuclear MDSC recruitment and enhances viral immunotherapy in pancreatic cancer. *Cell Mol Immunol* 22, 282-299. 10.1038/s41423-025-01260-3.
  20. Jensen, C.B., Pyke, C., Rasch, M.G., Dahl, A.B., Knudsen, L.B., and Secher, A. (2018). Characterization of the Glucagonlike Peptide-1 Receptor in Male Mouse Brain Using a Novel Antibody and In Situ Hybridization. *Endocrinology* 159, 665-675. 10.1210/en.2017-00812.
  21. Pyke, C., and Knudsen, L.B. (2013). The glucagon-like peptide-1 receptor--or not? *Endocrinology* 154, 4-8. 10.1210/en.2012-2124.
  22. Sriram, K., Wiley, S.Z., Moyung, K., Gorr, M.W., Salmeron, C., Marucut, J., French, R.P., Lowy, A.M., and Insel, P.A. (2019). Detection and Quantification of GPCR mRNA: An Assessment and Implications of Data from High-Content Methods. *ACS Omega* 4, 17048-17059. 10.1021/acsomega.9b02811.
  23. Ayoubi, R., Ryan, J., Biddle, M.S., Alshafie, W., Fotouhi, M., Bolivar, S.G., Ruiz Moleon, V., Eckmann, P., Worrall, D., McDowell, I., et al. (2023). Scaling of an antibody validation procedure enables quantification of antibody performance in major research applications. *eLife* 12. 10.7554/eLife.91645.

24. Michel, M.C., Wieland, T., and Tsujimoto, G. (2009). How reliable are G-protein-coupled receptor antibodies? *Naunyn Schmiedebergs Arch Pharmacol* 379, 385-388. 10.1007/s00210-009-0395-y.
25. Ast, J., Broichhagen, J., and Hodson, D.J. (2021). Reagents and models for detecting endogenous GLP1R and GIPR. *EBioMedicine* 74, 103739. 10.1016/j.ebiom.2021.103739.
26. Drucker, D.J. (2016). Never Waste a Good Crisis: Confronting Reproducibility in Translational Research. *Cell metabolism* 24, 348-360. 10.1016/j.cmet.2016.08.006.
27. Drucker, D.J. (2024). Efficacy and Safety of GLP-1 Medicines for Type 2 Diabetes and Obesity. *Diabetes care* 47, 1873-1888. 10.2337/dci24-0003.
28. Cummings, J.L., Atri, A., Feldman, H.H., Hansson, O., Sano, M., Knop, F.K., Johannsen, P., Leon, T., and Scheltens, P. (2025). evoke and evoke+: design of two large-scale, double-blind, placebo-controlled, phase 3 studies evaluating efficacy, safety, and tolerability of semaglutide in early-stage symptomatic Alzheimer's disease. *Alzheimers Res Ther* 17, 14. 10.1186/s13195-024-01666-7.